

Tensor Correlations Measured in ${}^3\text{He}(e, e'pp)n$

H. Baghdasaryan,^{26, *} L.B. Weinstein,^{26, †} J.M. Laget,³² K.P. Adhikari,²⁶ M. Aghasyan,¹⁵ M. Amarian,²⁶ M. Anghinolfi,¹⁶ H. Avakian,^{32, 15} J. Ball,⁶ M. Battaglieri,¹⁶ I. Bedlinskiy,¹⁹ B.L. Berman,¹³ A.S. Biselli,^{10, 27} C. Bookwalter,¹² W.J. Briscoe,¹³ W.K. Brooks,^{34, 32} S. Bültmann,²⁶ V.D. Burkert,³² D.S. Carman,³² V. Crede,¹² A. D'Angelo,^{17, 29} A. Daniel,²⁵ N. Dashyan,³⁸ R. De Vita,¹⁶ E. De Sanctis,¹⁵ A. Deur,³² B. Dey,⁴ R. Dickson,⁴ C. Djalali,³¹ G.E. Dodge,²⁶ D. Doughty,^{7, 32} R. Dupre,¹ H. Egiyan,^{23, 37} A. El Alaoui,¹ L. El Fassi,¹ P. Eugenio,¹² S. Fegan,³⁵ M.Y. Gabrielyan,¹¹ G.P. Gilfoyle,²⁸ K.L. Giovanetti,²⁰ W. Gohn,⁸ R.W. Gothe,³¹ K.A. Griffioen,³⁷ M. Guidal,¹⁸ L. Guo,¹¹ V. Gyurjyan,³² H. Hakobyan,^{34, 38} C. Hanretty,¹² C.E. Hyde,²⁶ K. Hicks,²⁵ M. Holtrop,²³ Y. Iieva,³¹ D.G. Ireland,³⁵ K. Joo,^{8, 36} D. Keller,²⁵ M. Khandaker,²⁴ P. Khetarpal,²⁷ A. Kim,²¹ W. Kim,²¹ A. Klein,²⁶ F.J. Klein,^{5, 32} P. Konczykowski,⁶ V. Kubarovskiy,³² S.E. Kuhn,²⁶ S.V. Kuleshov,^{34, 19} V. Kuznetsov,²¹ N.D. Kvaltine,³⁶ K. Livingston,³⁵ H.Y. Lu,⁴ I. J. D. MacGregor,³⁵ N. Markov,⁸ M. Mayer,²⁶ J. McAndrew,⁹ B. McKinnon,³⁵ C.A. Meyer,⁴ K. Mikhailov,¹⁹ V. Mokeev,^{30, 32} B. Moreno,⁶ K. Moriya,⁴ B. Morrison,² H. Moutarde,⁶ E. Munevar,¹³ P. Nadel-Turonski,³² C. Nepali,²⁶ S. Niccolai,¹⁸ G. Niculescu,^{20, 25} I. Niculescu,^{20, 13} M. Osipenko,¹⁶ A.I. Ostrovidov,¹² R. Paremuzyan,³⁸ K. Park,^{32, 21} S. Park,¹² E. Pasyuk,^{32, 2} S. Anefalos Pereira,¹⁵ S. Pisano,¹⁸ O. Pogorelko,¹⁹ S. Pozdniakov,¹⁹ J.W. Price,³ S. Procureur,⁶ D. Protopopescu,³⁵ G. Ricco,¹⁶ M. Ripani,¹⁶ G. Rosner,³⁵ P. Rossi,¹⁵ F. Sabatié,^{6, 26} C. Salgado,²⁴ R.A. Schumacher,⁴ H. Seraydaryan,²⁶ G.D. Smith,³⁵ D.I. Sober,⁵ D. Sokhan,¹⁸ S.S. Stepanyan,²¹ S. Stepanyan,³² P. Stoler,²⁷ S. Strauch,³¹ M. Taiuti,¹⁶ W. Tang,²⁵ C.E. Taylor,¹⁴ D.J. Tedeschi,³¹ M. Ungaro,⁸ M.F. Vineyard,^{33, 28} E. Voutier,²² D.P. Watts,⁹ D.P. Weygand,³² M.H. Wood,³⁹ B. Zhao,³⁷ and Z.W. Zhao³⁶

(The CLAS Collaboration)

¹Argonne National Laboratory, Argonne, Illinois 60441

²Arizona State University, Tempe, Arizona 85287-1504

³California State University, Dominguez Hills, Carson, CA 90747

⁴Carnegie Mellon University, Pittsburgh, Pennsylvania 15213

⁵Catholic University of America, Washington, D.C. 20064

⁶CEA, Centre de Saclay, Irfu/Service de Physique Nucléaire, 91191 Gif-sur-Yvette, France

⁷Christopher Newport University, Newport News, Virginia 23606

⁸University of Connecticut, Storrs, Connecticut 06269

⁹Edinburgh University, Edinburgh EH9 3JZ, United Kingdom

¹⁰Fairfield University, Fairfield CT 06824

¹¹Florida International University, Miami, Florida 33199

¹²Florida State University, Tallahassee, Florida 32306

¹³The George Washington University, Washington, DC 20052

¹⁴Idaho State University, Pocatello, Idaho 83209

¹⁵INFN, Laboratori Nazionali di Frascati, 00044 Frascati, Italy

¹⁶INFN, Sezione di Genova, 16146 Genova, Italy

¹⁷INFN, Sezione di Roma Tor Vergata, 00133 Rome, Italy

¹⁸Institut de Physique Nucléaire ORSAY, Orsay, France

¹⁹Institute of Theoretical and Experimental Physics, Moscow, 117259, Russia

²⁰James Madison University, Harrisonburg, Virginia 22807

²¹Kyungpook National University, Daegu 702-701, Republic of Korea

²²LPSC, Université Joseph Fourier, CNRS/IN2P3, INPG, Grenoble, France

²³University of New Hampshire, Durham, New Hampshire 03824-3568

²⁴Norfolk State University, Norfolk, Virginia 23504

²⁵Ohio University, Athens, Ohio 45701

²⁶Old Dominion University, Norfolk, Virginia 23529

²⁷Rensselaer Polytechnic Institute, Troy, New York 12180-3590

²⁸University of Richmond, Richmond, Virginia 23173

²⁹Università di Roma Tor Vergata, 00133 Rome Italy

³⁰Skobeltsyn Nuclear Physics Institute, Skobeltsyn Nuclear Physics Institute, 119899 Moscow, Russia

³¹University of South Carolina, Columbia, South Carolina 29208

³²Thomas Jefferson National Accelerator Facility, Newport News, Virginia 23606

³³Union College, Schenectady, NY 12308

³⁴Universidad Técnica Federico Santa María, Casilla 110-V Valparaíso, Chile

³⁵University of Glasgow, Glasgow G12 8QQ, United Kingdom

³⁶University of Virginia, Charlottesville, Virginia 22901

³⁷College of William and Mary, Williamsburg, Virginia 23187-8795

³⁸*Yerevan Physics Institute, 375036 Yerevan, Armenia*

³⁹*Canisius College, Buffalo, NY 14208*

(Dated: October 31, 2018)

We have measured the ${}^3\text{He}(e, e'pp)n$ reaction at an incident energy of 4.7 GeV over a wide kinematic range. We identified spectator correlated pp and pn nucleon pairs using kinematic cuts and measured their relative and total momentum distributions. This is the first measurement of the ratio of pp to pn pairs as a function of pair total momentum, p_{tot} . For pair relative momenta between 0.3 and 0.5 GeV/c, the ratio is very small at low p_{tot} and rises to approximately 0.5 at large p_{tot} . This shows the dominance of tensor over central correlations at this relative momentum.

PACS numbers: 21.45.-v 25.30.Dh

In order to understand the structure of the nucleus, we need to understand both the independent motion of individual nucleons and the corrections to that simple picture. Single nucleon momentum distributions have been measured in electron-proton knockout reactions, $(e, e'p)$, and are reasonably well understood [1–3]. However, only about 70% of the naively expected number of protons are seen. The missing 30% are presumably due to nucleons in short range and long range correlations.

These nucleon-nucleon (NN) correlations are the next important ingredient. A ${}^{12}\text{C}(p, ppn)$ experiment [4] found that low momentum neutrons, $p_n < 0.22$ GeV/c, were emitted isotropically but that high momentum neutrons were emitted opposite to the struck proton's missing momentum, \vec{p}_{miss} , and were therefore the correlated partner of the struck protons.

Measurements of the cross section ratios of inclusive electron scattering from nuclei relative to deuterium, $\sigma[A(e, e')]/\sigma[d(e, e')]$, together with calculations of deuterium show that the momentum distributions for $p > 0.25$ GeV/c have the same shape for all nuclei and that nucleons have between a 5% and a 25% probability of being part of a correlated pair [5–8].

Thus, when a nucleon has low momentum, $p < p_{fermi}$, its momentum is balanced by the rest of the nucleus; however, when $p > p_{fermi}$, its momentum is almost always balanced by only one other nucleon and the two nucleons form a correlated pair. These correlated pairs are responsible for the high momentum parts of the nuclear wave function [7]. Note that these correlations can be caused by either the central ($L = 0$) or the tensor ($L = 2$) parts of the NN force.

Nucleons in nuclei overlap each other a significant fraction of the time. These high momentum correlated pairs should be at significantly higher local density than the nuclear average. Thus, understanding correlated NN pairs will improve our understanding of cold dense nuclear matter, neutron stars [9], and the EMC effect [10].

Recent measurements of direct two nucleon knockout from carbon using protons [11] and electrons [12, 13] have shown that the removal of a proton from the nucleus with $0.275 < p_{miss} < 0.550$ GeV/c is almost always accompanied by the emission of a correlated nucleon that carries momentum roughly equal and opposite to \vec{p}_{miss} and that

this nucleon is almost always a neutron. Quantitative interpretations are complicated by the presence of other effects, including Final State Interactions (FSI) and two-body currents such as meson exchange currents (MEC), which add coherently to the correlations signal [14].

A recent measurement of ${}^3\text{He}(e, e'pp)n$ [15] isolated the NN correlated pairs by knocking out the third nucleon and observing the momenta of the spectator nucleons. It measured the pp and pn relative and total momentum distributions. Because the virtual photon was absorbed on the third nucleon, the correlated pairs were spectators and thus the effects of two-body currents were negligible. However, the continuum interaction of the spectator pair significantly reduced the cross sections and therefore complicated the theoretical calculations [16–18]. Thus, this type of measurement complements the direct knockout measurements.

This paper reports new ${}^3\text{He}(e, e'pp)n$ results at higher energy and higher momentum transfer that provide a cleaner measurement of two-nucleon momentum distributions over a wide range of correlated pair total and relative momenta.

We measured ${}^3\text{He}(e, e'pp)n$ at Jefferson Lab in 2002 using a 100% duty factor, 5–10 nA beam of 4.7 GeV electrons incident on a 5-cm liquid ${}^3\text{He}$ target. We detected the outgoing charged particles in the CEBAF Large Acceptance Spectrometer (CLAS) [19].

CLAS uses a toroidal magnetic field and six sets of drift chambers, time-of-flight scintillation counters and electro-magnetic calorimeters (EC) for particle identification and trajectory reconstruction. The polar angular acceptance is $8^\circ < \theta < 140^\circ$ and the azimuthal acceptance is 50% at smaller polar angles, increasing to 80% at larger polar angles. The EC was used for the electron trigger with a threshold of ≈ 0.9 GeV. Regions of non-uniform detector response were excluded by software cuts, while acceptance and tracking efficiencies were estimated using GSIM, the CLAS GEANT Monte-Carlo simulation. Protons were detected down to $p_p \geq 0.25$ GeV/c. $\text{H}(e, e'p)$ was measured and compared to the world's data [20] to determine our electron and proton detection efficiencies [21].

We identified electrons using the energy deposited in the EC, and protons using time-of-flight. We identified

the neutron using missing mass to select ${}^3\text{He}(e, e'pp)n$ events. We eliminated target wall interactions by selecting particles originating in the central 4-cm of the target. Fig. 1 shows the electron kinematics ($Q^2 = \vec{q}^2 - \omega^2$, ω is the energy transfer, and \vec{q} is the three-momentum transfer) and missing mass distribution. For ${}^3\text{He}(e, e'pp)n$ events, the momentum transfer Q^2 peaks at around $1.5 (\text{GeV}/c)^2$. ω is concentrated slightly above but close to quasielastic kinematics ($\omega = Q^2/2m_p$).

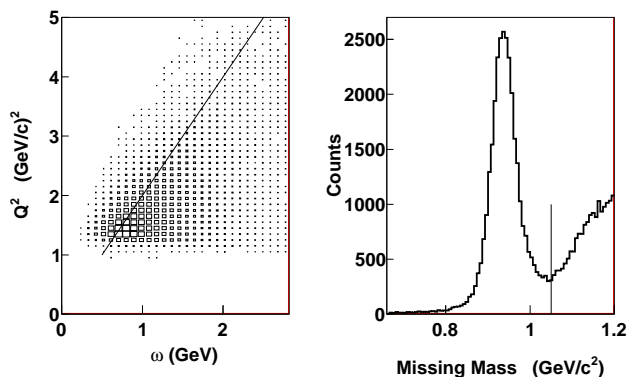


FIG. 1: a) Q^2 vs. ω for ${}^3\text{He}(e, e'pp)n$ events. The line shows the quasielastic condition $\omega = Q^2/2m_p$. Note the large acceptance. b) Missing mass for ${}^3\text{He}(e, e'pp)X$. The vertical line indicates the neutron missing mass cut.

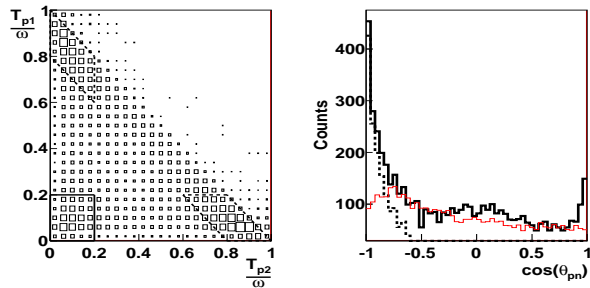


FIG. 2: a) ${}^3\text{He}(e, e'pp)n$ lab frame ‘‘Dalitz plot.’’ T_{p1}/ω vs. T_{p2}/ω for events with $p_N > 0.25 \text{ GeV}/c$. The solid lines indicate the ‘leading n plus pp pair’ and the dashed lines indicate the ‘leading p plus pn pair’ selection cuts. b) The cosine of the pn lab frame opening angle for events with a leading p and a pn pair. The thick solid line shows the uncut data, the dashed line shows the data cut on $p_{\perp}^{\text{leading}} < 0.3 \text{ GeV}/c$, and the thin solid line (color online) shows the uncut three-body absorption simulation (with arbitrary normalization).

To understand the energy sharing in the reaction, we plotted the lab frame kinetic energy of the first proton divided by the energy transfer (T_{p1}/ω) versus that of the second proton (T_{p2}/ω) for events with nucleon momenta p_p and $p_n > 0.25 \text{ GeV}/c$ (see Fig. 2a). (The

assignment of protons 1 and 2 is arbitrary. Events with $T_{p1}/\omega + T_{p2}/\omega > 1$ are non-physical and are due to the experimental resolution.) There are three peaks at the three corners of the plot, corresponding to events where two nucleons each have less than 20% of ω and the third ‘leading’ nucleon has the remainder. We selected these peaks, as shown in Fig. 2a.

Fig. 2b shows the opening angle for pn pairs with a leading proton (the pp pair opening angle is almost identical). Note the large peak at 180° . The peak is not due to the cuts, since we do not see it in a simulation of three-body absorption of the virtual photon followed by phase space decay [22]. It is also not due to the CLAS acceptance since we see it for both pp and pn pairs. This back-to-back peak is a very strong indication of correlated NN pairs.

Now that we have identified correlated pairs, we want to study them. To reduce the effects of final state rescattering, we required the perpendicular momentum (relative to \vec{q}) of the leading nucleon, $p_{\perp}^{\text{leading}} < 0.3 \text{ GeV}/c$. The resulting NN pair opening angle distribution is almost entirely back-to-back (see Fig. 2b). The neutron of the pn pair is distributed almost isotropically with respect to \vec{q} . The pair average total momentum parallel to \vec{q} ($\sim 0.1 \text{ GeV}/c$) is also much smaller than the average momentum transfer ($\sim 1.6 \text{ GeV}/c$). These show that the NN pairs are predominantly spectators and that their measured momentum distribution reflects their initial momentum distribution.

The resulting lab frame relative $\vec{p}_{\text{rel}} = (\vec{p}_1 - \vec{p}_2)/2$ and total $\vec{p}_{\text{tot}} = \vec{p}_1 + \vec{p}_2$ momenta of the NN pairs are shown in Fig. 3. The cross sections are integrated over the experimental acceptance. Radiative and tracking efficiency corrections have been applied [21]. The systematic uncertainty is 15%, primarily due to the uncertainty in the low momentum proton detection efficiency.

The pp and pn pair momentum distributions are similar to each other. The p_{rel} distributions rise rapidly starting at $\approx 0.25 \text{ GeV}/c$ (limited by $p_N \geq 0.25 \text{ GeV}/c$), peak at $\approx 0.4 \text{ GeV}/c$, and have a tail extending to $\approx 0.7 \text{ GeV}/c$. The p_{tot} distributions rise rapidly from zero, peak at $\approx 0.25 \text{ GeV}/c$, and fall rapidly. Both distributions have an upper limit determined by the cut $T_N/\omega \leq 0.2$. These distributions are also similar for both data sets ($Q^2 \sim 0.7$ [15] and 1.5 GeV^2). The $Q^2 \sim 1.5 \text{ GeV}^2$ pp p_{rel} distribution peaks at slightly larger momentum than either the pn or lower Q^2 data.

We also compared our data to a one-body calculation by Golak, integrated over the experimental acceptance, that includes an ‘exact’ calculation of the fully correlated initial state wave function (wf), absorption of the virtual photon by the leading nucleon and ‘exact’ calculations of the continuum wf of the spectator NN pair [23]. The calculation does not treat the rescattering of the leading nucleon. Including the continuum wf of the NN pair (*i.e.*, not treating those two outgoing nucleons as plane

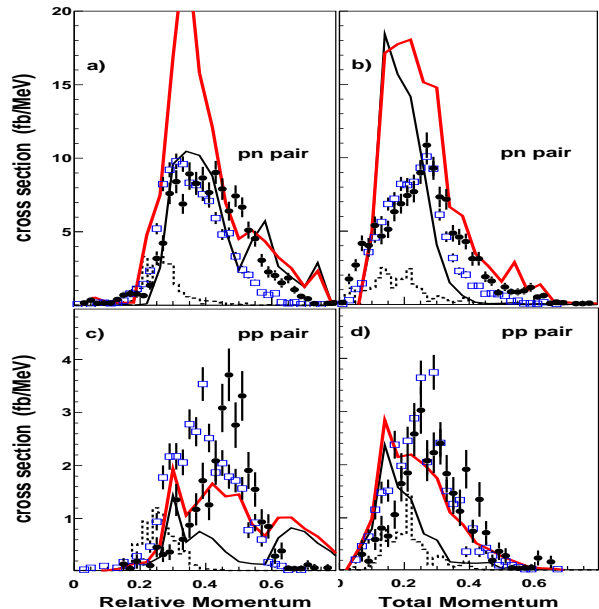


FIG. 3: a) Cross section vs. pn pair p_{rel} . Solid points show these data ($Q^2 \sim 1.5 \text{ GeV}^2$), open squares (blue online) show $Q^2 \sim 0.7 \text{ GeV}^2$ data [15], dashed histogram shows the Golak one-body calculation [23], thin solid line shows the Laget one-body calculation and the thick solid line (red online) shows the Laget full calculation [18, 24, 25]; b) the same for p_{tot} ; c) and d) the same for pp pairs. All quantities are in the lab frame. The $Q^2 \sim 0.7 \text{ GeV}^2$ data have been reduced by a factor of 5.3 (the ratio of the cross sections) for comparison.

waves) reduces the cross section by about an order of magnitude. Note that this calculation is not strictly valid for $p_{rel} > 0.35 \text{ GeV}/c$ (the pion production threshold). This calculation significantly underestimates the data.

The one-body calculation of Laget [18, 24, 25], using a diagrammatic approach, sees the same large cross section reduction due to the NN pair continuum wf. His one-body calculation describes the pn pair p_{rel} distribution well. Laget’s full calculations also indicate large three-body current (MEC or IC) contributions for both pn and pp pairs. His three-body currents improve the agreement for pp pairs and worsen the agreement for pn pairs.

The ratio of pp to pn spectator pair integrated cross sections is about 1:4. This is approximately consistent with the product of the ratio of the number of pairs and σ_{ep}/σ_{en} , the ratio of the elementary ep and en cross sections for pn and pp pairs. This ratio appears inconsistent with the pp to pn pair ratio of 1:18 measured in direct pair knockout in $^{12}\text{C}(e, e'pN)$ [13] at $0.3 < p_{rel} < 0.5 \text{ GeV}/c$ and at relatively low $p_{tot} (< 0.15 \text{ GeV}/c)$.

In order to study this apparent discrepancy we calculated the ratio of the pp to pn cross sections integrated over $0.3 < p_{rel} < 0.5 \text{ GeV}/c$ as a function of p_{tot} (see Fig. 4). The ratio has been multiplied by 1.5 to ap-

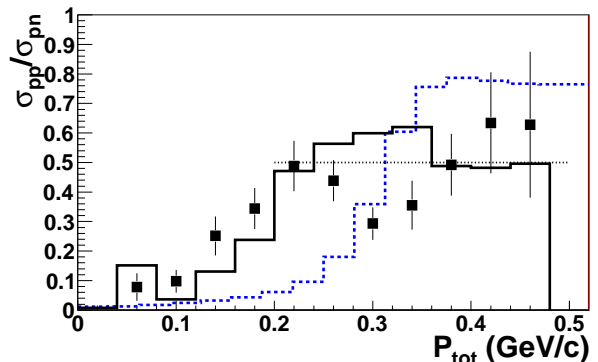


FIG. 4: Ratio of pp to pn spectator pair cross sections, integrated over $0.3 < p_{rel} < 0.5 \text{ GeV}/c$. The points show the data, the solid histogram shows the Golak one-body calculation [23] and the dashed histogram (color online) shows the ratio of the Golak pp and pn bound state momentum distributions. The dotted line at 0.5 shows the simple-minded pair counting result. The data and the one-body calculation have been multiplied by 1.5 to approximately account for the ratio of the average ep and en elementary cross sections.

proximately account for the ratio of the average ep and en cross sections. The ratio is very small for $p_{tot} < 0.1 \text{ GeV}/c$, consistent with the $^{12}\text{C}(e, e'pN)$ results, and increases to 0.4–0.6 for $p_{tot} > 0.2 \text{ GeV}/c$. The measured ratio increases starting at $p_{tot} \sim 0.1 \text{ GeV}/c$, in contrast with that calculated from the bound state wf, which increases starting at around $0.3 \text{ GeV}/c$. The ratio is consistent with Golak’s one-body calculation. The ratio at large p_{tot} is also consistent with simple pair counting.

This increase in the pp to pn ratio with p_{tot} is a signal for the dominance of tensor correlations. At low p_{tot} , where the angular momentum of the pair with respect to the rest of the nucleus must be zero, the pp pairs predominantly have (isospin, spin) $(T, S) = (1, 0)$ [26]. They are in an s -state, which has a minimum at $p_{rel} \sim 0.4 \text{ GeV}/c$. The pn pair is predominantly in a deuteronlike $(T, S) = (0, 1)$ state. Due to the tensor interaction, the pn pair has a significant d -state admixture and does not have this minimum [26–28]. This leads to a small ratio at small p_{tot} . As p_{tot} increases, the minimum in the pp p_{rel} distribution fills in, increasing the pp to pn ratio.

To summarize, we have measured the $^3\text{He}(e, e'pp)n$ reaction at an incident energy of 4.7 GeV over a wide kinematic range, centered at $Q^2 \sim 1.5 \text{ GeV}^2$ and $w \approx Q^2/2m_p$. We selected events with one leading nucleon and a spectator correlated NN pair by requiring that the spectator nucleons each have less than 20% of the transferred energy and that the leading nucleon’s momentum perpendicular to \vec{q} be less than $0.3 \text{ GeV}/c$. The p_{rel} and p_{tot} distributions for spectator pp and pn pairs are very similar to each other and to those measured at lower momentum transfer. The ratio of pp to pn pair

cross sections for $0.3 < p_{rel} < 0.5$ GeV/c is very small at low p_{tot} and rises to approximately 0.5 at large p_{tot} . Since pp pairs at low p_{tot} are in an s -state, this ratio shows the dominance of tensor over central correlations.

We acknowledge the outstanding efforts of the staff of the Accelerator and Physics Divisions (especially the CLAS target group) at Jefferson Lab that made this experiment possible. This work was supported in part by the Italian Istituto Nazionale di Fisica Nucleare, the Chilean CONICYT, the French Centre National de la Recherche Scientifique and Commissariat à l’Energie Atomique, the UK Science and Technology Facilities Council (STFC), the U.S. Department of Energy and National Science Foundation, and the National Research Foundation of Korea. Jefferson Science Associates, LLC, operates the Thomas Jefferson National Accelerator Facility for the United States Department of Energy under contract DE-AC05-06OR23177.

* Current address: University of Virginia, Charlottesville, Virginia 22901

† Contact Author weinstein@odu.edu

- [1] S. Frullani and J. Mougey, *Adv. Nucl. Phys.* **14**, 1 (1984).
- [2] J. Kelly, *Adv. Nucl. Phys.* **23**, 75 (1996).
- [3] J. Gao et al., *Phys. Rev. Lett.* **84**, 3265 (2000).
- [4] A. Tang et al., *Phys. Rev. Lett.* **90**, 042301 (2003).
- [5] K. Egiyan et al., *Phys. Rev. C* **68**, 014313 (2003).
- [6] K. Egiyan et al., *Phys. Rev. Lett.* **96**, 082501 (2006).
- [7] A. Antonov, P. Hodgson, and I. Petkov, *Nucleon Momentum and Density Distributions in Nuclei* (Clarendon Press, 1988).
- [8] J. Forest et al., *Phys. Rev. C* **54**, 646 (1996).
- [9] L. Frankfurt and M. Strikman (AIP, 2008), vol. 1056, pp. 241–247.
- [10] M. M. Sargsian et al., *J. Phys.* **G29**, R1 (2003).
- [11] E. Piassetzky et al., *Phys. Rev. Lett.* **97**, 162504 (2006).
- [12] R. Shneor et al., *Phys. Rev. Lett.* **99**, 072501 (2007).
- [13] R. Subedi et al., *Science* **320**, 1476 (2008).
- [14] S. Janssen et al., *Nucl. Phys.* **A672**, 285 (2000).
- [15] R. Niyazov et al., *Phys. Rev. Lett.* **92**, 052303 (2004).
- [16] W. Glöckle et al., *Acta Phys. Polon.* **B32**, 3053 (2001).
- [17] C. Ciofi degli Atti and L.P. Kaptari, *Phys. Rev. C* **66**, 044004 (2002).
- [18] J.M. Laget, *Phys. Rev. C* **35**, 832 (1987).
- [19] B. Mecking et al., *Nucl. Inst. and Meth.* **A503**, 513 (2003).
- [20] J. Arrington, *Phys. Rev. C* **68**, 034325 (2003).
- [21] H. Baghdasaryan, Ph.D. thesis, ODU (2007).
- [22] K. Hagiwara et al., *Phys. Rev. D* **66**, 010001 (2002).
- [23] J. Golak et al., *Phys. Rev. C* **51**, 1638 (1995).
- [24] J.M. Laget, *J. Phys. G* **14**, 1445 (1988).
- [25] J. M. Laget, *Phys. Lett.* **B609**, 49 (2005).
- [26] R. Schiavilla, R. B. Wiringa, S. C. Pieper, and J. Carlson, *Physical Review Letters* **98**, 132501 (2007).
- [27] M. M. Sargsian, T. V. Abrahamyan, M. I. Strikman, and L. L. Frankfurt, *Phys. Rev. C* **71**, 044615 (2005).
- [28] M. Alvioli, C. Ciofi degli Atti, and H. Morita, *Phys. Rev. Lett.* **100**, 162503 (2008).